"Brain on Fire": Hyperperfusion as a Hallmark of Hyperammonemic Encephalopathy

Sameer Peer[1] Paramdeep Singh[1] Ritish Gupta[1] Priya Bhat[2]

[1] Department of Radiodiagnosis, All India Institute of Medical Sciences, Bathinda, Punjab, India
[2] Department of Microbiology, Adesh Institute of Medical Sciences, Bathinda, Punjab, India

Address for correspondence Dr. Paramdeep Singh, MD, Department of Radiodiagnosis, All India Institute of Medical Sciences, Bathinda 151001, Punjab, India (e-mail: paramdeepdoctor@gmail.com).

Ann Natl Acad Med Sci (India) 2023;59:225–228.

Abstract

We describe a very rare case of acute fulminant hepatic failure as a complication of acute viral hepatitis caused by hepatitis A virus, complicated by hyperammonemic encephalopathy. The brain magnetic resonance imaging (MRI) findings were suggestive of cytotoxic edema involving bilateral cerebral hemispheres. The novel findings of hyperperfusion on arterial spin labeling perfusion MRI and hyperemic hypoxia on susceptibility weighted imaging are discussed. The patient had a rapid progression of cerebral edema and succumbed to the illness despite supportive care. Characteristic neuroimaging findings may help in the diagnosis of acute hyperammonemic encephalopathy of brain MRI, which may be useful in leading to appropriate clinical workup and diagnosis of the underlying cause of hyperammonemia. In our case, hyperammonemic encephalopathy was precipitated by fulminant hepatic failure caused by hepatitis A virus, which is a rare occurrence.

Keywords
- hepatic encephalopathy
- hyperammonemia
- hepatitis

Introduction

Fulminant acute hepatic failure (FAHF) is a rare clinical syndrome characterized by rapidly progressive hepatic dysfunction that has a very high case fatality rate of the order of 50 to 70%.[1,2] Drug overdose (such as acetaminophen), viral hepatitis, alcohol abuse, and toxin exposure account for most of the cases of fulminant hepatic failure reported in the published literature. FAHF is an extremely rare complication of viral hepatitis caused by hepatitis A virus (HAV).[1] HAV, a picornavirus, is spread by the fecal–oral route and usually leads to a self-limiting acute hepatitis, which confers a lifelong immunity to the infected person. FAHF has been reported in less than 1% of patients infected with HAV. Patients with FAHF develop acute hepatic encephalopathy, markedly raised serum bilirubin levels, coagulopathy, and transaminitis (of the order of >1,000 U/L). Development of acute hepatic encephalopathy has been postulated to be due to accumulation of toxins within the blood, which are normally handled by metabolism in the liver.[3] Hyperammonemia has been reported to be the most implicated cause for acute hepatic encephalopathy. Hyperammonemic encephalopathy has a characteristic neuroimaging phenotype, which is distinct from hypoxic and other toxic encephalopathies and, in relevant clinical setting, may be pathognomonic of acute hyperammonemic encephalopathy.[4] Herein we report of case of acute encephalopathy in which neuroimaging findings led to a diagnosis of acute hyperammonemia, which was subsequently found to be due to HAV-associated FAHF. Our case is unique as we report the findings of arterial spin labeling (ASL) magnetic resonance imaging (MRI) perfusion

article published online
December 18, 2023

DOI https://doi.org/10.1055/s-0043-1777315.
ISSN 0379-038X.

Thieme Medical and Scientific Publishers Pvt. Ltd., A-12, 2nd Floor, Sector 2, Noida-201301 UP, India

in acute hyperammonemic encephalopathy due to HAV-associated FAHF. To the best of our knowledge, such findings have not been reported in the published literature.

Case Description

A 17-year-old adolescent girl was brought to the emergency department of our institution after she was found unconscious after a brief febrile illness of 2 days' duration. There was no history suggestive of any previous comorbid illness. The bystanders did not report any seizure or trauma. There was no fecal or urinary incontinence and no tongue bite. On examination, the patient was found to be in altered sensorium with a Glasgow Coma Scale (GCS) score of 9/15. The clinical examination was remarkable for icterus. The abdominal examination was within normal limits. Review of systems did not reveal any significant abnormality. There was no history suggestive of drug overdose or toxin intake. The following vitals were recorded at presentation: heart rate of 110 beats per minute (regular), respiratory rate of 22/min (irregular), SPO_2 of 93% on room air, and blood pressure of 140/90 mm Hg.

Considering the patient was in acute encephalopathy with reduced GCS, MRI of the brain was done, which revealed diffuse symmetric edema involving the cerebral cortex in both the cerebral hemispheres, manifesting as a cortical swelling and hyperintense signal on T2-weighted (T2W) image (►**Fig. 1a**) and fluid attenuated inversion recovery (FLAIR) images (►**Fig. 1b**). Effacement of the sulcal spaces and basal cisterns was noted (►**Fig. 1c**). Bilateral uncal herniation was evident (►**Fig. 1d**). Diffusion weighted images revealed

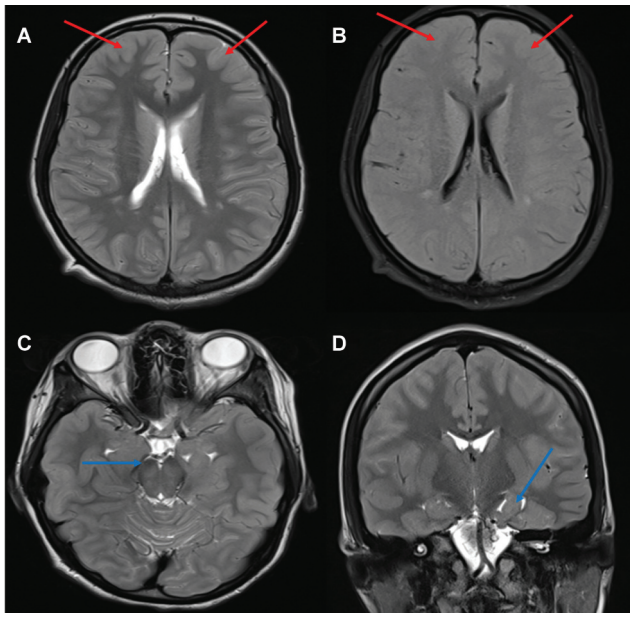

Fig. 1 Magnetic resonance imaging (MRI) of the brain. (**A**) Axial T2-weighted (T2W) image shows diffuse cortical edema in bilateral frontal lobes (*red arrows*). (**B**) Axial fluid attenuated inversion recovery (FLAIR) image shows hyperintense signal in the involved cortex with loss of gray–white differentiation (*red arrows*). (**C**) Axial T2W image shows effacement of the basal cisterns (*blue arrow*). (**d**) Coronal T2W image shows left-sided uncal herniation (*blue arrow*).

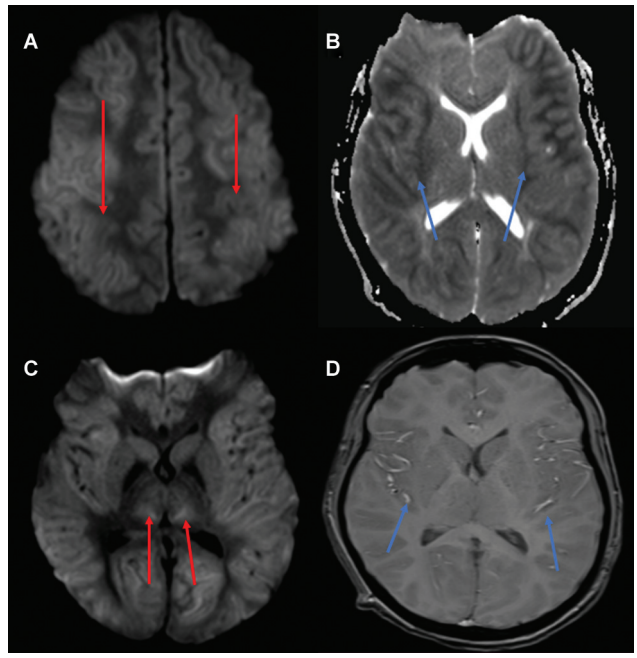

Fig. 2 Magnetic resonance imaging (MRI) of the brain. (**A**) Axial diffusion weighted image shows cortical diffusion restriction with relative sparing of bilateral peri-Rolandic regions (*red arrows*). (**B**) Axial apparent diffusion coefficient (ADC) map shows symmetric cortical and juxtacortical cytotoxic edema involving the insular region (*blue arrows*). (**C**) Symmetric diffusion restriction noted in bilateral thalami on axial diffusion weighted image (*red arrows*). (**D**) Axial susceptibility weighted image (SWI) shows hyperintense signal in cortical veins (*blue arrows*), suggestive of hyperemic hypoxia in the setting of cytotoxic edema.

cortical diffusion restriction, characterized by involvement of the bilateral insula and cingulate gyri with relative sparing of bilateral peri-Rolandic cortex and parieto-occipital regions (►**Fig. 2a**). On apparent diffusion coefficient (ADC) maps, symmetric hypointense signal involving the cortex and juxtacortical white matter was noted corresponding to the areas of diffusion restriction (►**Fig. 2b**). These findings suggested diffuse cytotoxic edema. Symmetric cytotoxic edema was also noted in bilateral thalami (►**Fig. 2c**). Sparing of the cerebellum, brainstem, and basal ganglia was noted (►**Fig. 2d**). On susceptibility weighted images (SWI), relative hyperintense signal was noted in cerebral arteries as well as cortical veins (►**Fig. 2e**), indicating reduced cerebral oxygen extraction due to cytotoxic edema and subsequent increased concentration of oxyhemoglobin in the cortical veins. No hemorrhages were noted. ASL MRI perfusion revealed diffusely increased perfusion in the bilateral cerebral cortices, corresponding to the areas involved on T2W, FLAIR, and DWI sequences (►**Fig. 3**). Considering the typical neuroimaging findings and the pattern of involvement, a diagnosis of acute hyperammonemic encephalopathy was considered. The patient was intubated and managed with intravenous (IV) mannitol and lactulose administered through a nasogastric tube.

Laboratory investigations showed total serum bilirubin level of 10.8 mg/dL, alkaline phosphatase level of 320 U/L, alanine aminotransferase (ALT) level of 1,400 U/L, and aspartate aminotransferase level of 1,700 U/L. Prothrombin time was noted to

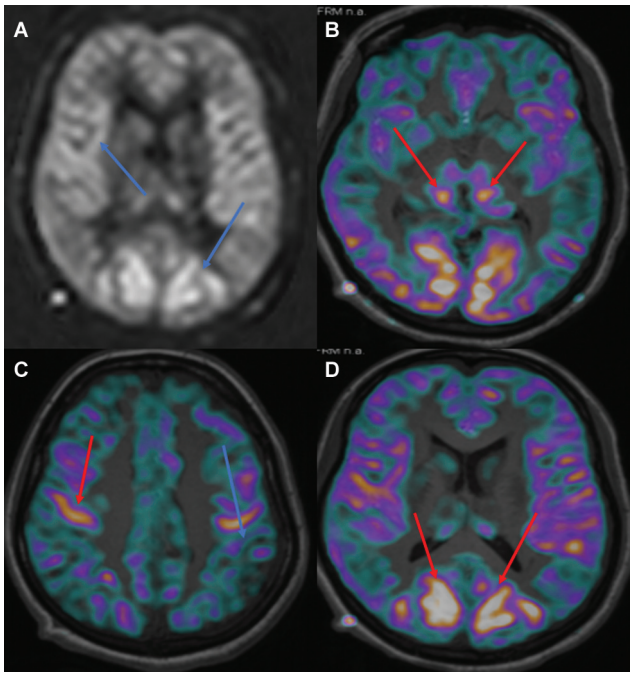

Fig. 3 Perfusion weighted images using arterial spin labeling. (**A**) Grayscale arterial spin labeling (ASL) image shows bilateral symmetric cortical hyperperfusion (*blue arrows*). (**B**) Fused ASL T1-weighted (T1W) image shows symmetric hyperperfusion in bilateral thalami (*red arrows*). (**C**) Fused ASL-T1W image shows hyperperfusion in precentral gyrus (*red arrow*) with relatively reduced perfusion in postcentral gyrus (*blue arrow*). (**D**) Axial fused ASL-T1W image shows bilaterally symmetric hyperperfusion in bilateral occipital lobes (*red arrows*).

be 65 seconds and international normalized ratio (INR) of 4.5. Blood sugars and renal functions were within normal range. Serum immunoglobulin M (IgM) for HAV was found to show significantly high titers. Serum ammonia level was noted to be 114 µmol/L. Arterial blood gas analysis revealed the presence of metabolic acidosis with pH of 7.2 (normal range: 7.35–7.45), $PaCO_2$ of 33 mm Hg (normal range: 35–45 mm Hg), bicarbonate level of 18 mmol/L (21–28 mmol/L), and PaO_2 of 92 mm Hg (normal range of 80–100 mm Hg). Thus, a final diagnosis of FAHF caused by acute viral hepatitis complicated by acute hepatic encephalopathy was made. The patient had a rapid deterioration of symptoms. She did not respond to supportive measures and ultimately succumbed to the illness within 3 days of hospital admission.

Discussion

Hyperammonemia leads to encephalopathy by various mechanisms. In the cases with acute liver failure, serum ammonia levels rise. The increased ammonia levels result in increased influx of ammonia into the astrocytes, both the active transport of quaternary ammonium ions and diffusion of ammonia through the blood–brain barrier. Within the astrocytes, the elevated levels of ammonia and ammonium ions lead to osmotic derangements resulting in swelling of the astrocytes.[5] Another proposed mechanism includes alteration in sodium-potassium pump function, uptake of glutamine, potassium, pyruvate, and lactate within the astrocytes and excitotoxicity mediated with increased extracellular glutamate levels, which activate the N-methyl-D-aspartate (NMDA) receptors.[6] Hyperammonemia may result from hepatic causes (such as acute or chronic liver failure), portosystemic shunting (such as after transjugular intrahepatic portosystemic shunt procedure), and urea cycle disorders.[7] Hyperammonemic encephalopathy in the setting of FAHF secondary to HAV infection is extremely rare.[1] The alterations in cerebral blood flow in hyperammonemic encephalopathy have been investigated in various publications with varying results. While most of the previous publications suggest a reduction in the cerebral blood flow (CBF) in cases of hyperammonemic encephalopathy, few publications have shown elevated CBF, particularly in type B hepatic encephalopathy, which results from portosystemic shunting.[8,9] In one of the studies reporting ASL findings in hyperammonemic encephalopathy due to urea cycle disorders, initial hypoperfusion was followed by hyperperfusion.[10] In the index case, profound increase in CBF was noted on ASL in the acute phase. These findings are in correspondence with the presence of cytotoxic cerebral edema. The cytotoxic state results in reduced oxygen utilization in the brain, which probably results in compensatory increase in CBF.[11] In our case, these findings are corroborated by the findings on SWI, which shows an increase in intracranial venous signal due to reduced utilization of oxygen by brain and thus increase in oxyhemoglobin concentration in the venous blood, a state that may be referred to as hyperemic hypoxia.[12]

Although the neuroimaging findings were characteristic of hyperammonemic encephalopathy in the index case, few differential diagnoses need to be considered in such cases presenting with encephalopathy. Status epilepticus may result in similar findings of diffuse cytotoxic edema and hyperperfusion with hyperemic hypoxia.[13] However, the clinical scenario excluded convulsive seizure. Still, nonconvulsive status epilepticus needs to be kept in the differential diagnosis. Hypoxic encephalopathy in adults could result in diffuse cortical cytotoxic edema; however, peri-Rolandic involvement and cerebellar and basal ganglia involvement are usually seen in hypoxic–ischemic encephalopathy.[14] Osmotic demyelination may show changes of cytotoxic edema in pontine and extrapontine distribution; however, basal ganglia involvement is characteristic in extrapontine forms of osmotic demyelination.[15] Also, clinical scenario of rapid correction of hyponatremia is suggestive of the diagnosis in such cases. Hypoglycemic encephalopathy in adults is suggested by cytotoxic edema involving the basal ganglia and cerebral cortex, in particular, parieto-occipital and insular involvement. In adults with hypoglycemic encephalopathy, the cerebellum and brainstem are spared. Diffusion restriction in bilateral corona radiata has also been described in hypoglycemic encephalopathy.[16] On the other hand, hyperglycemic encephalopathy may be encountered in diabetic ketoacidosis and is characterized by diffuse cytotoxic cerebral edema. However, the diagnosis is usually evident by clinical and laboratory parameters.[17] Posterior reversible encephalopathy syndrome (PRES) is characterized by bilaterally symmetrical edema involving the parieto-occipital

region and may involve the cerebellum and brainstem. In typical cases, no diffusion restriction is seen. Pattern of hypoperfusion is commonly encountered in PRES, although some cases of hyperperfusion have also been described.[18]

Conclusion

We have described an exceedingly rare complication of HAV infection wherein the patient developed rapidly progressive hyperammonemic encephalopathy following FAHF. Characteristic neuroimaging findings have been described. We emphasize on diffuse hyperperfusion in the cerebral cortex in the setting of cytotoxic edema, exquisitely depicted by ASL perfusion. Also, the findings of hyperemic hypoxia on SWI reinforce the hypothesis of reduced cerebral oxygen utilization in the setting of cytotoxic edema in this case. To the best of our knowledge, such findings are novel and have not been described previously in a case of HAV-associated FAHF and hyperammonemic encephalopathy.

Ethics Statement

The authors declare that the manuscript conforms to the Declarations of Helsinki. Informed written consent was taken from the guardians of the patient for data acquisition and publication.

Authors' Contribution

S.P. contributed to drafting of the manuscript and data acquisition. P.S. contributed to data acquisition, and approval of the final draft of the manuscript. R.G. contributed to drafting of the manuscript and approval of the final draft of the manuscript. P.B. contributed to data collection and approval of the final draft of the manuscript.

Conflict of Interest

None declared.

References

1 Shammout R, Alhassoun T, Rayya F. Acute liver failure due to hepatitis A virus. Case Rep Gastroenterol 2021;15(03):927–932
2 Rovegno M, Vera M, Ruiz A, Benítez C. Current concepts in acute liver failure. Ann Hepatol 2019;18(04):543–552
3 Jayakumar AR, Norenberg MD. Hyperammonemia in hepatic encephalopathy. J Clin Exp Hepatol 2018;8(03):272–280
4 Reis E, Coolen T, Lolli V. MRI findings in acute hyperammonemic encephalopathy: three cases of different etiologies—teaching point: to recognize MRI findings in acute hyperammonemic encephalopathy. J Belg Soc Radiol 2020;104(01):9
5 Tranah TH, Paolino A, Shawcross DL. Pathophysiological mechanisms of hepatic encephalopathy. Clin Liver Dis (Hoboken) 2015;5 (03):59–63
6 Llansola M, Rodrigo R, Monfort P, et al. NMDA receptors in hyperammonemia and hepatic encephalopathy. Metab Brain Dis 2007;22(3-4):321–335
7 Auron A, Brophy PD. Hyperammonemia in review: pathophysiology, diagnosis, and treatment. Pediatr Nephrol 2012;27(02): 207–222
8 Larsen FS. Cerebral blood flow in hyperammonemia: heterogeneity and starling forces in capillaries. Metab Brain Dis 2002;17(04): 229–235
9 Bjerring PN, Gluud LL, Larsen FS. Cerebral blood flow and metabolism in hepatic encephalopathy: a meta-analysis. J Clin Exp Hepatol 2018;8(03):286–293
10 Sen K, Whitehead MT, Gropman AL. Multimodal imaging in urea cycle-related neurological disease: what can imaging after hyperammonemia teach us? Transl Sci Rare Dis 2020;5(1–2):87–95
11 Siwicka-Gieroba D, Robba C, Gołacki J, Badenes R, Dabrowski W. Cerebral oxygen delivery and consumption in brain-injured patients. J Pers Med 2022;12(11):1763
12 Verma RK, Abela E, Schindler K, et al. Focal and generalized patterns of cerebral cortical veins due to non-convulsive status epilepticus or prolonged seizure episode after convulsive status epilepticus: a MRI study using susceptibility weighted imaging. PLoS One 2016;11(08):e0160495
13 Ko SB, Ortega-Gutierrez S, Choi HA, et al. Status epilepticus-induced hyperemia and brain tissue hypoxia after cardiac arrest. Arch Neurol 2011;68(10):1323–1326
14 Muttikkal TJ, Wintermark M. MRI patterns of global hypoxic-ischemic injury in adults. J Neuroradiol 2013;40(03):164–171
15 Garg P, Aggarwal A, Malhotra R, Dhall S. Osmotic demyelination syndrome - evolution of extrapontine before pontine myelinolysis on magnetic resonance imaging. J Neurosci Rural Pract 2019; 10(01):126–135
16 Ren S, Chen Z, Liu M, Wang Z. The radiological findings of hypoglycemic encephalopathy: a case report with high b value DWI analysis. Medicine (Baltimore) 2017;96(43):e8425
17 Barrot A, Huisman TA, Poretti A. Neuroimaging findings in acute pediatric diabetic ketoacidosis. Neuroradiol J 2016;29(05): 317–322
18 Fazeli S, Noorbakhsh A, Imbesi SG, Bolar DS. Cerebral perfusion in posterior reversible encephalopathy syndrome measured with arterial spin labeling MRI. Neuroimage Clin 2022;35:103017

